Available online at www.sciencedirect.com
ScienceDirect
Analytical Biochemistry 375 (2008) 282–290
ANALYTICAL BIOCHEMISTRY
www.elsevier.com/locate/yabio

Studies of the binding and signaling of surface-immobilized periplasmic glucose receptors on gold nanoparticles: A glucose biosensor application

Silvana Andreescu [a,*], Linda A. Luck [b]

[a] Department of Chemistry and Biomolecular Science, Clarkson University, Potsdam, NY 13699, USA
[b] Department of Chemistry, State University of New York at Plattsburgh, Plattsburgh, NY 12901, USA

Received 21 November 2007
Available online 8 January 2008

Abstract

Genetically engineered periplasmic glucose receptors as biomolecular recognition elements on gold nanoparticles (AuNPs) have allowed our laboratory to develop a sensitive and reagentless electrochemical glucose biosensor. The receptors were immobilized on AuNPs by a direct sulfur–gold bond through a cysteine residue that was engineered in position 1 on the protein sequence. The study of the attachment of genetically engineered and wild-type proteins binding to the AuNPs was first carried out in colloidal gold solutions. These constructs were studied and characterized by UV–Vis spectroscopy, transmission electron microscopy, particle size distribution, and zeta potential. We show that the genetically engineered cysteine is important for the immobilization of the protein to the AuNPs. Fabrication of the novel electrochemical biosensor for the detection of glucose used these receptor-coated AuNPs. The sensor showed selective detection of glucose in the micromolar concentration range, with a detection limit of 0.18 μM.

Keywords: Gold nanoparticles; Biofunctionalization; Periplasmic glucose/galactose receptor; Biosensor; Surface immobilization; Self-assembled protein monolayers

During the past decade, gold nanoparticles (AuNPs)[1] have attracted an enormous amount of attention in the scientific and engineering fields due to their multifaceted properties. Recently, they have been widely used in combination with proteins, peptides, enzymes, antibodies, and nucleic acids [1–10]. These biomolecule–AuNP assemblies have found applications in biotechnology, biology, and medicine for the development of biological assays and biolabeling, in drug delivery, and as probes in cancer detection. Immobilization of proteins in a functional state on AuNPs is of critical importance in practical applications, especially in biosensing and biolabeling [7–10].

Here we describe studies that incorporate genetically engineered periplasmic binding proteins that sense glucose on the surface of AuNPs. We further describe an electrochemical methodology to utilize these protein–AuNP assemblies for use in biosensors to detect glucose in the micromolar range. For the most part, biosensors use target molecules that are immobilized on or within a suitable material that is in direct contact with the surface of a transducer. AuNPs are an ideal platform for biosensors, especially for those with electrochemical detection, because the gold surface area is suitable for binding of biomolecules and the metal facilitates direct and fast electron transfer.

* Corresponding author. Fax: +1 315 268 6610.
E-mail address: eandrees@clarkson.edu (S. Andreescu).

[1] *Abbreviations used:* AuNP, gold nanoparticle; GGR, glucose/galactose receptor; GGR–WT, glucose/galactose receptor–wild type; GGR–Cys, glucose/galactose receptor where alanine was replaced by cysteine at the N-terminal position; ζ-potential, zeta potential; PSD, particle size distribution; TEM, transmission electron microscopy; PB, phosphate buffer; DI, deionized water; HR–TEM, high-resolution transmission electron microscopy; GCE, glassy carbon electrode; SEM, scanning electron microscopy; CV, cyclic voltammetry.

0003-2697/$ - see front matter © 2007 Elsevier Inc. All rights reserved.
doi:10.1016/j.ab.2007.12.035

Moreover, the AuNPs, as compared with flat gold surfaces, have a much higher surface area, allowing the loading of a larger amount of protein and potentially more sensitivity [7–10]. For many biosensor applications in the literature, the biomolecules are attached to gold surfaces via thiol linkers attached on the gold surface [11,12] or, as in the current study, are directly linked to the gold by the use of sulfur atoms within the bioentity [13,14]. The receptors used in a number of studies from our laboratories have used a cysteine residue endogenous to the native protein, or one that is genetically engineered into the protein. This can be used to link and spatially orient the biomolecule on the gold surface [15–22]. When a surface-exposed cysteine residue on a protein is not feasible, thiol linkers to other residues on a protein allow semispecifically oriented layers on the surface [23]. Although there has been some discussion in the literature pointing to protein deposition without exposed cysteines, a number of studies from our laboratories have indicated that native glucose/galactose receptors (GGRs) without a genetically engineered cysteine residue do not bind to the gold surface, whereas receptors with a surface-exposed cysteine form a stable affinity bond to gold surfaces [15–22].

The current study was undertaken to explore the oriented immobilization of receptor proteins to AuNPs. For our purposes of developing a glucose biosensor, we used the periplasmic glucose/galactose receptor–wild type (GGR–WT), which is highly specific for its natural cognate ligands. Ligand binding is accompanied by a large conformational change [15]. GGR–WT has no native cysteines, but we have developed a number of mutants that have one surface-exposed cysteine residue that can be used to attach the protein to a gold surface. For this study, we used the mutant where alanine was replaced by cysteine at the N-terminal position (GGR–Cys). This engineered site provides an SH group for protein linkage to the gold surfaces. The advantage of such an approach is the precise control and orientation of the protein on the electrode surface with the preservation of its functional properties. This system circumvents the denaturation or instability problems commonly encountered when immobilization is achieved through physical adsorption or covalent linkage of natural proteins.

A number of studies have been reported using the GGR and genetically engineered cysteine mutants of this receptor where we have looked at detected binding through changes in surface plasmon resonance [17], frequency decrease on a quartz crystal microbalance [15], change in rigidity by atomic force microscopy [22], and electrochemical impedance [18,21]. In the current study, the AuNPs with immobilized receptor proteins are characterized by UV–Vis spectroscopy, zeta potential (ζ-potential), particle size distribution (PSD), and transmission electron microscopy (TEM). We demonstrate the utility of these AuNPs as a means to detect glucose in the micromolar range. In addition, this study serves as a model for the development of electrochemical biosensors using receptors that bind to small molecules. Applicability of this system could be extended to a number of protein families, including the steroid hormone receptor superfamily, and to the detection of xenoestrogens.

Materials and methods

Expression and purification of recombinant proteins

The preparation and expression of GGR–WT and GGR–Cys have been described previously [17]. Fig. 1 illustrates the position of the amino acid cysteine mutation and the orientation of the protein on the nanoparticle.

Reagents and solutions

$HAuCl_4$ $3H_2O$ (23.03 wt% Au, 6.5 wt% free HCl) was purchased from Degussa (South Plainfield, NJ, USA). Isoascorbic acid ($C_6H_8O_6$) was obtained from Fluka. The phosphate buffer (PB) solution (pH 6.5) used for the preparation of 10 mM $K_3[Fe(CN)_6]$ (Fischer Scientific, Fair Lawn, NJ, USA) contains 0.1 M KH_2PO_4 (Fischer Scientific) and 0.1 M Na_2HPO_4 (J. T. Baker, Phillipsburg, NJ,

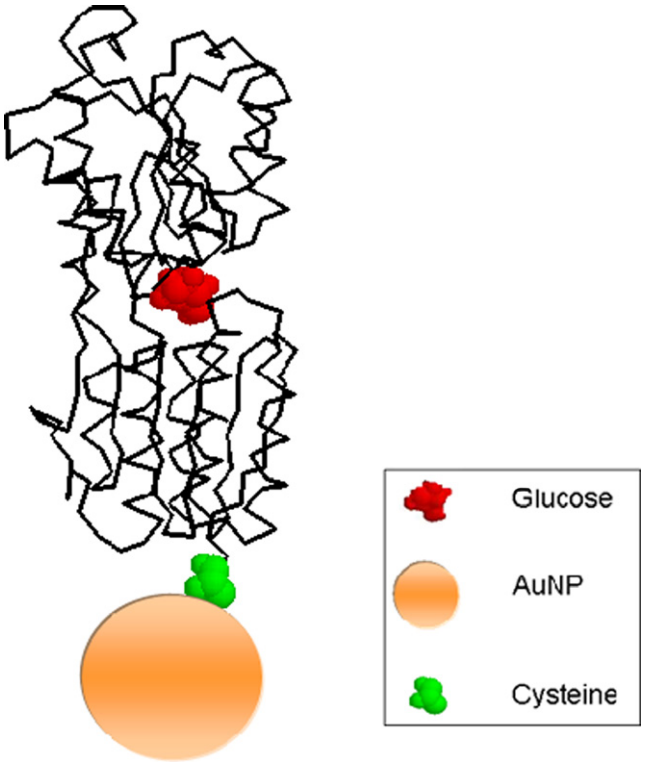

Fig. 1. Backbone structure of the glucose and galactose binding protein attached to the AuNP. This figure illustrates the position of the alanine to cysteine mutation at position 1 in green and the glucose in the binding pocket in red. The drawing was done using PDB file 2GBP from the Protein Data Bank. The nanoparticle is not drawn to scale because it actually is 10 times larger than the protein. (For interpretation of the references to color in this figure legend, the reader is referred to the Web version of this article.)

USA). All aqueous solutions were prepared with deionized water (DI) using a Millipore Direct-Q system with a resistivity of 18.2 MΩ. D-Glucose, fructose, L-valine, and L-leucine were purchased from Sigma. Protein buffer contained 100 mM KCl, 10 mM Tris (pH 7.1), and 0.5 $CaCl_2$ (Tris buffer). Tris buffer was used in all experiments involving colloidal gold in the presence/absence of proteins.

Instrumentation

The UV–Vis spectra of AuNPs were recorded with a Shimadzu P2041 spectrophotometer equipped with a 1-cm path length cell. The electrokinetic properties, ζ-potential, and PSD were measured with a Brookhaven Zeta Plus–Zeta Potential Analyzer at 25 °C and calculated with standard software. The size, size distribution, and morphology of the AuNPs were measured by high-resolution transmission electron microscopy (HR–TEM) using a JEOL 2010 HR–TEM.

All electrochemical measurements were performed with a PARSTAT 2263 electrochemical analyzer (Princeton Applied Research) equipped with Power Suite software. These electrochemical experiments were carried out using a conventional cell operating with an Ag/AgCl/3M NaCl as reference electrode, a platinum wire as counterelectrode, and a glassy carbon electrode (GCE) with a geometrical surface area of 28 mm^2 as working electrode. The cell and electrodes all were provided by Bioanalytical Systems (West Lafayette, IN, USA).

Preparation of gold colloids

Gold colloids were obtained by reduction of gold ions with isoascorbic acid as described previously [24]. All glassware used in the preparation of AuNPs was cleaned in an HNO_3 bath, rinsed thoroughly with distilled water, and dried prior to use. A stable red gold colloidal solution was obtained. The resulting AuNPs are uniform and highly dispersed, with an average particle diameter between 30 and 40 nm (as determined by TEM and scanning electron microscopy [SEM] analysis) [24]. The absence of dispersing agents during the preparation procedure ensures a clean gold surface, making them attractive for further modification with biomolecules.

Preparation of protein–AuNP conjugates: Study of protein attachment

The protein production and genetic engineering of the native glucose and galactose protein and the mutant used in this study were described previously [17]. For the current article, we have defined the native protein as GGR–WT and the alanine to cysteine mutant of GGR as GGR–Cys. An illustration of the position of this mutation and its binding on an AuNP is given in Fig. 1. The point of attachment of the cysteine residue is far from the glucose binding site in the GGR protein; thus, this modification has no effect on its binding capability.

The immobilization of both GGR–WT and GGR–Cys to the AuNPs was accomplished by mixing 0.84 ml of 0.2 mM colloidal gold solution with 0.14 ml of 7 μM protein solution. The solutions were stirred for approximately 20 to 30 s and then analyzed by UV–Vis spectroscopy and ζ-potential. The results were compared with the spectra of a control colloidal gold solution in the absence of protein. To evaluate the immobilization of the proteins on the AuNPs, the conjugates were separated by centrifugation (15 min at 6000 rpm) and the UV–Vis spectrum of the supernatant was recorded to check for the presence of proteins. For HR–TEM analysis, one drop of gold or protein-modified AuNP colloidal solution without sonication was deposited on a TEM copper grid and dried under vacuum.

Electrode preparation and electrochemical studies

AuNPs were deposited on the surface of a GCE by electrodeposition from a gold solution. The procedure involves applying a constant potential of −200 mV for 60 s in a solution of 1.2 μM $HAuCl_4$. The solution was prepared in distilled water and deoxygenated by purging with N_2 for approximately 15 min. Prior to deposition, the GCE was cleaned and dried according to the following sequence: polish with 0.3 μm alumina powder, wash ultrasonically for 10 min in distilled water, rinse with distilled water, and dry under a nitrogen stream. The surface of the electrode prior to and after deposition of proteins was characterized by cyclic voltammetry (CV) using the model reversible redox couple $Fe^{II}(CN)_6^{4-}/Fe^{III}(CN)_6^{3-}$. For this purpose, the three electrodes were immersed in a classical electrochemical cell containing $K_3Fe(CN)_6$, 10 mM prepared in PB (pH 6.5), and the potential was scanned between 0 and 0.6 V versus Ag/AgCl reference electrode at a scan rate of 50 mV/s.

Biosensor fabrication and binding studies

The GCE–AuNP electrodes prepared by electrochemical deposition were incubated in 0.5 ml of 7 μM GGR–WT (or GGR–Cys) for 1 h at room temperature. The electrodes were rinsed thoroughly with Tris buffer to remove the excess of unbound protein and were incubated in D-glucose solution at a given concentration. D-Fructose, L-valine, and L-leucine were used as negative controls because they are not natural ligands and do not bind to the protein. Protein immobilization, as well as the binding of target ligands, was evaluated by CV using $Fe(CN)_6^{3-}/Fe(CN)_6^{4-}$ solution (10 mM) in PB (pH 6.5) by scanning the potential between 0 and 0.6 V at a scan rate of 100 mV/s. For evaluation of nonspecific absorption of the protein, attachment of GGR–WT and subsequent binding of glucose were performed under the same experimental conditions as for GGR–Cys.

Results and discussion

Study of binding and activity of recombinant proteins on AuNPs

UV–Vis spectroscopy

It is known that highly dispersed gold colloids (single particles) in solution present a single absorption peak attributed to quadrupole plasmon excitation [25]. The position of the plasmon absorption band depends on the size, surface properties, mutual interactions in the dispersion medium, and extent of aggregation. The attachment of the proteins on AuNPs and the surface changes due to the absorbed proteins are expected to affect the surface plasmon. This results in a color change in the solution [26]. Aggregation of AuNPs usually is observed as a red shift in the color arising from the absorption bands at long wavelengths due to coupling between plasmons of neighboring particles inside the aggregates. In general, the smaller the interparticle distance, the larger the red shift [27]. The gold sols prepared in our preparations of Au^{3+} with isoascorbic acid have a red wine color and a well-defined absorbance peak at approximately 523 nm [24]. The stability of these electrostatically stabilized sols is highly dependent on the ionic strength of the system. Because very small additions of salts might cause coagulation of the AuNPs, we first studied the effect of the Tris buffer solution (pH 7.1) in which the proteins were prepared on the UV–Vis spectrum. The spectrum presents a well-defined peak at approximately 523 nm and a small wide shoulder starting at approximately 650 nm (Fig. 2A). The small peaks at approximately 226 and 320 nm are attributed to the square planar $AuCl_4^-$ complex ion. This spectrum was used as a control in the absence of proteins.

In the presence of proteins, gold colloidal particles form aggregates. On protein binding, the absorbance usually shifts to higher wavelength as the aggregation proceeds [24,25]. In our experiment, in the presence of GGR–WT, there was an increase in the gold peak at 523 nm, concomitant with the appearance of a new peak at 280 nm corresponding to the protein (Fig. 2A). No color change in the gold sols was observed. Thus, the wild-type protein does not bind to the gold particles.

In the presence of GGR–Cys, the color of the gold sol turned from red to blue, suggesting aggregation of the AuNPs due to the immobilized protein on their surface. The UV–Vis spectrum of the gold sols containing 1 μM GGR–Cys shows very distinct characteristics, with the peak corresponding to the AuNPs at 523 nm shifting to 600 nm and the new peak being significantly broader (Fig. 2A). In addition, there was no noticeable peak at 280 nm, suggesting that all of the protein in solution is attached to the AuNPs. The protein coating of the gold particles induces aggregation between the AuNPs, thereby producing changes in the plasmon absorption band associated with the color change.

The GGR–WT and GGR–Cys have distinctly different effects on the AuNPs that are more evident after 24 h of incubation of AuNPs and protein. After this time, the color of the solution and the characteristics of the UV–Vis spectrum of the GGR–WT did not change significantly. In contrast, the mixture of GGR–Cys and the AuNPs formed visible bluish aggregates that precipitated, leaving the supernatant nearly colorless. The UV–Vis spectrum in Fig. 2B illustrates this phenomenon. After centrifugation and separation, no protein was present in the supernatant in the case of GGR–Cys, suggesting that all of the protein was attached on the nanoparticles that formed large aggregates. Our spectrophotometric measurement showed that the total amount GGR–WT was retrieved in the supernatant, proving that the wild-type protein without the genetically engineered cysteine did not bind to the AuNPs under our experimental conditions.

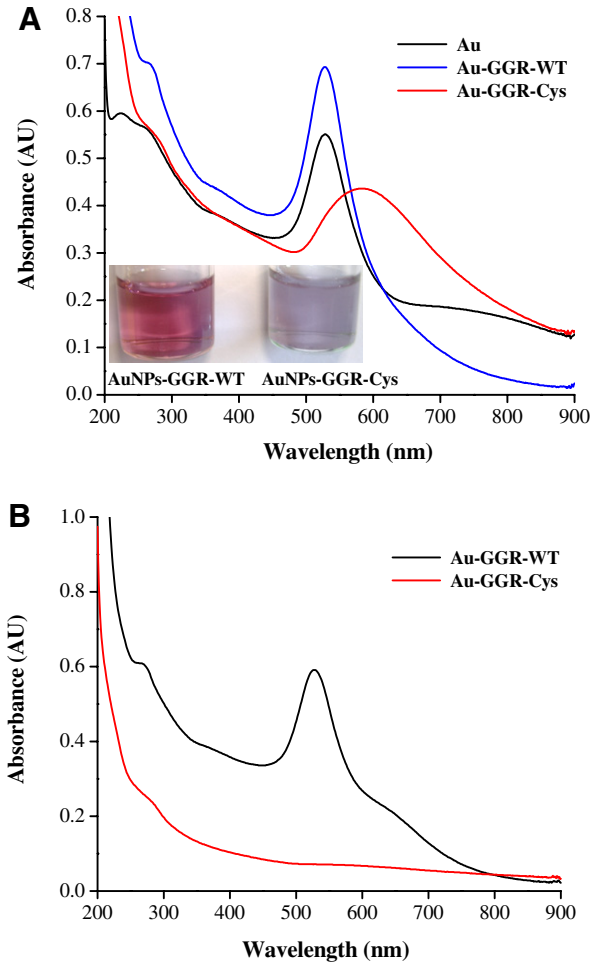

Fig. 2. UV–Vis spectra of AuNPs in the absence (Au) and presence of GGR–WT (Au_GGR–WT) and GGR–Cys (Au_GGR–Cys) immediately after mixing (A) and after 48 h incubation (B). In all experiments, a 10-mM Tris buffer solution (pH 7.1) containing 100 mM KCl and 0.5 mM $CaCl_2$ was used. Panel A inset: Color of gold sols in the presence of GGR–WT and GGR–Cys. AU, arbitrary units.

ζ-Potential and TEM analysis

HR–TEM and ζ-potential analysis was used to characterize the surface properties, morphology, and size distribu-

tion of the AuNPs with and without immobilized protein. The surface modification can affect the surface charge of nanoparticles; this determines the dispersion and/or aggregation of colloidal solution at a given pH value. The bare AuNPs used in this work were negatively charged, with an average ζ-potential value of -29.1 ± 4.1 mV. In the presence of GGR–WT, the ζ-potential value was -19.3 ± 2.0 mV, suggesting a partial modification of the AuNPs surface. When the GGR–Cys was added, the AuNPs were nearly neutral in charge (with a ζ-potential value of -4.25 ± 6.6 mV, indicating nearly complete coverage of the particles by a protein coating. The PSD of AuNPs in Tris buffer determined using the dynamic light scattering analyzer (Fig. 3A) indicates an average size of 42.5 nm. For the GGR–WT, the PSD shows an average diameter of 59.4 nm, whereas for the GGR–Cys, the average size of the aggregates formed was 139.6 nm.

These findings were also supported by the HR–TEM analysis. Fig. 4A shows the HR–TEM image of the bare AuNPs obtained by chemical precipitation of Au^{3+} with isoascorbic acid used for protein immobilization. As can be seen in the figure, the nanoparticles are quite uniform and monodispersed. The same behavior was observed when the GGR–WT protein was added to the solution. When GGR–Cys was used, the particles formed large aggregates (Fig. 3C). Analysis of a single AuNP + GGR–Cys at a lower magnification shows the presence of a thin layer on the surface of the particle. We speculate that this layer could be attributed to the protein, which is 35 Å wide and 65 Å long. The characteristics (ζ-potential, average particle size, UV–Vis peaks, and color) of the three configurations tested (AuNPs, AuNPs + GGR–WT, and AuNPs + GGR–Cys) are summarized in Table 1.

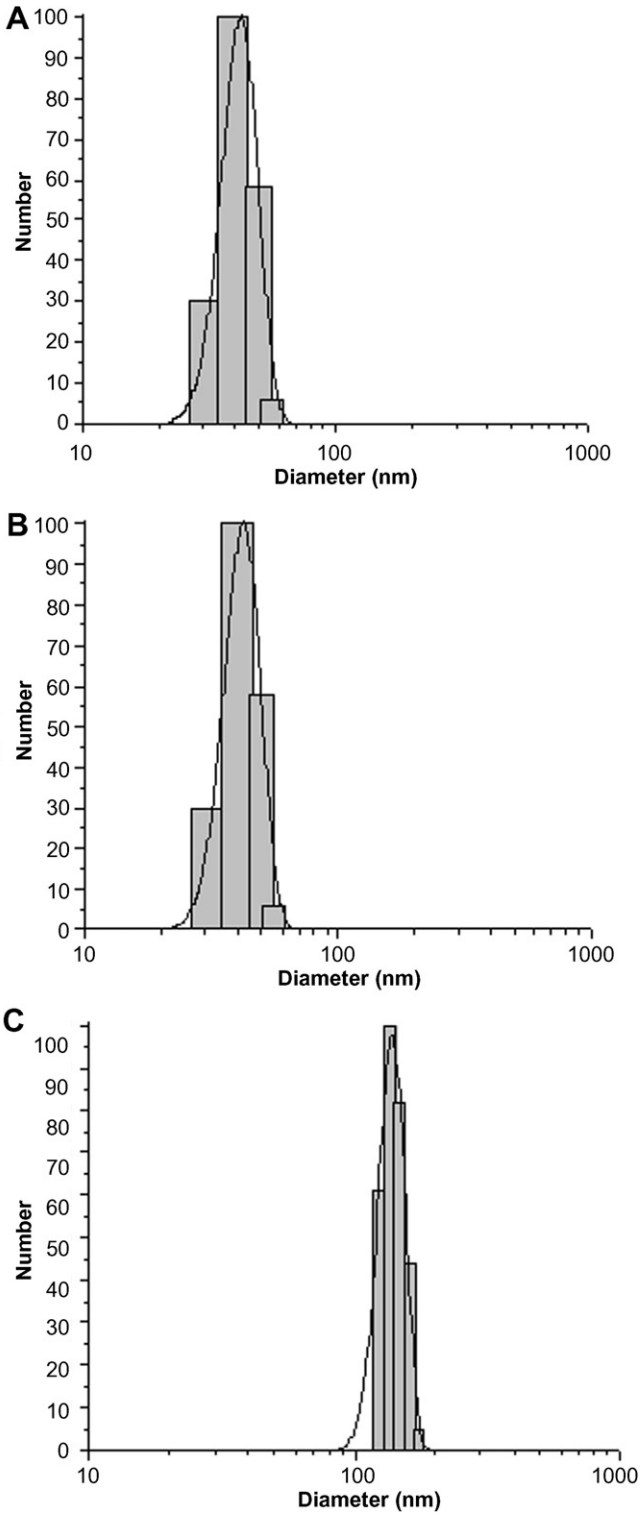

Fig. 3. PSD of AuNPs in the absence (A) and presence of GGR–WT (B) and GGR–Cys (C).

Fabrication of electrochemical biosensor for detection of glucose

The binding between the AuNPs and the two glucose receptor proteins was further investigated using CV after deposition of AuNPs on the surface of a working GCE. The recombinant proteins used in this work are engineered and act as an uptake system for a target ligand that in this case is glucose. The receptor binds D-glucose with a K_d of 0.1 μM. The binding of D-glucose produces a ligand-induced conformational change in the protein that is well characterized and has been used in a number of studies [15,17–19,23,26]. This specific binding, combined with the use of AuNPs for protein immobilization on an electrode surface, was employed in the current work in the construction of an electrochemical biosensor for the detection of glucose. A schematic of this experiment is illustrated in Fig. 5.

Biosensor fabrication

In our study, the AuNPs were electrodeposited on the GCE from a solution of $HAuCl_4$ according to a published literature procedure [28,29]. This resulted in a deposition of a smooth layer of aggregates of AuNPs that was confirmed by the change in the color of the working GCE surface from gray to yellow. The gold particles in the aggregate have an average size of approximately 50 nm, and this was also confirmed in our experiments by SEM (results not shown). This is in agreement with published literature

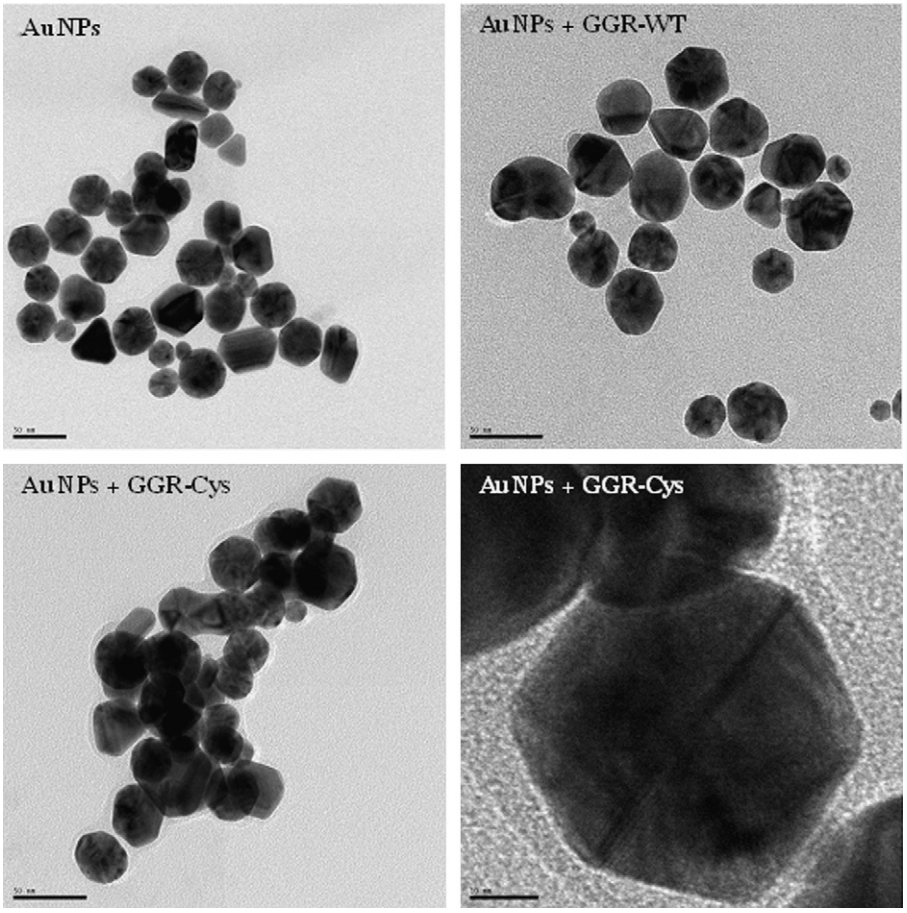

Fig. 4. TEM of AuNPs in the absence and presence of GGR–WT and GGR–Cys (scale = 50 nm). Different magnifications are shown for GGR–Cys (50 and 10 nm).

Table 1
Spectroscopic and morphological characteristics of AuNPs and AuNPs in the presence of GGR–WT and GGR–Cys

	ζ-Potential (mV)	Average size (nm)	UV–Vis peaks (nm)	Color/aggregation
AuNPs (Tris buffer)	−43.5 ± 4.1	42.5	523, 226, 320, and 650 (wide shoulder)	Red wine/Monodispersed particles
AuNPs + GGR–WT	−19.3 ± 2.0	59.4	523 and 280	Red wine/Monodispersed particles
AuNPs + GGR–Cys	−4.2 ± 6.6	139.6	600 (wide peak)	Blue/visible aggregates

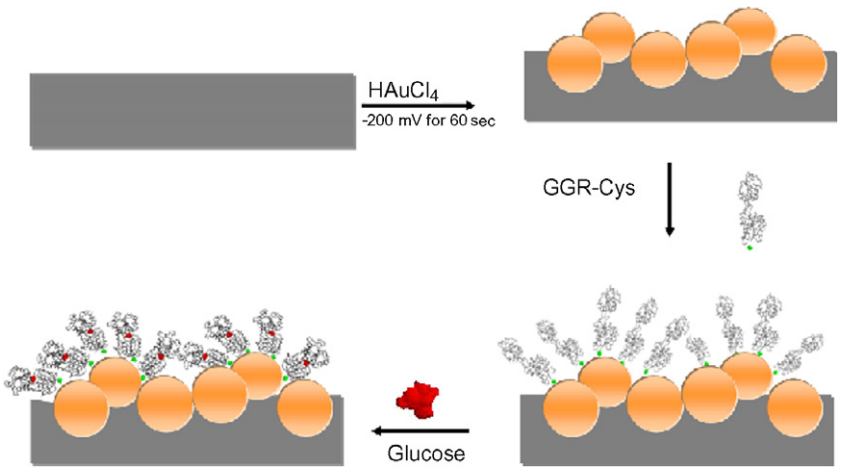

Fig. 5. Fabrication steps of the GCE–AuNP glucose sensor illustrating the binding of the protein via the cysteine residue on the GGR–Cys receptor and the subsequent glucose binding.

data [28,29]. The modified GCE–AuNP electrode was further characterized by CV using $Fe^{II}(CN)_6^{4-}/Fe^{III}(CN)_6^{3-}$ as a model redox probe. Compared with the bare GCE, the peak potential separation ΔE_p was reduced from 93 to 70 mV for the GCE–AuNPs. Concurrently, a current amplification of both anodic and cathodic peaks was observed, suggesting that the presence of gold promoted the electron transfer at the surface of the electrode (results not shown).

We used this system first to investigate whether the binding of the protein on the GCE–AuNP surface follows the same trend as in the case of colloidal particles and then to check the stability of the binding for both the wild-type and Cys modified protein. For this purpose, the protein (GGR–WT or GGR–Cys) was immobilized on the GCE–AuNP surface. Immobilization was carried out by incubating the gold modified electrode for 1 h in a solution containing protein at a concentration of 7 μM. The electrode was washed several times to remove the excess of weakly bound proteins. CV using the $Fe^{II}(CN)_6^{4-}/Fe^{III}(CN)_6^{3-}$ model reversible electrochemical reaction was then employed to characterize the electron transfer properties on the surface of the electrode before and after protein binding. It is expected that the GGR–Cys will attach to the gold surface through its Cys residue. This will partially insulate the electrochemically active surface, hampering the electron transfer of the redox probe. Fig. 6 represents the cyclic voltammogram obtained from the GCE–AuNP electrode with GGR–WT or GGR–Cys and without protein. The cyclic voltammogram recorded after exposure to GGR–WT is nearly identical to that corresponding with the bare GCE–AuNP electrode. This implies that there is little or no change on the surface of the AuNPs, suggesting that the WT protein does not bind to the electrode surface. In contrast, the exposure of GGR–Cys to the AuNPs induced a significant decrease in the oxidation and reduction peaks in the CV, clearly indicating the deposition of a protein layer that partially insulates the electrode surface. To confirm the role of the AuNPs, for comparison purposes, we performed similar studies with a conventional gold electrode. In the same experimental conditions, the electrochemical response of the gold electrode was significantly reduced (12.5 μA) as compared with that of the GCE–AuNPs (78 μA). After incubation in a solution of GGR–Cys, the protein binds to the Au electrode, but the decrease in the signal was very small (Fig. 6B).

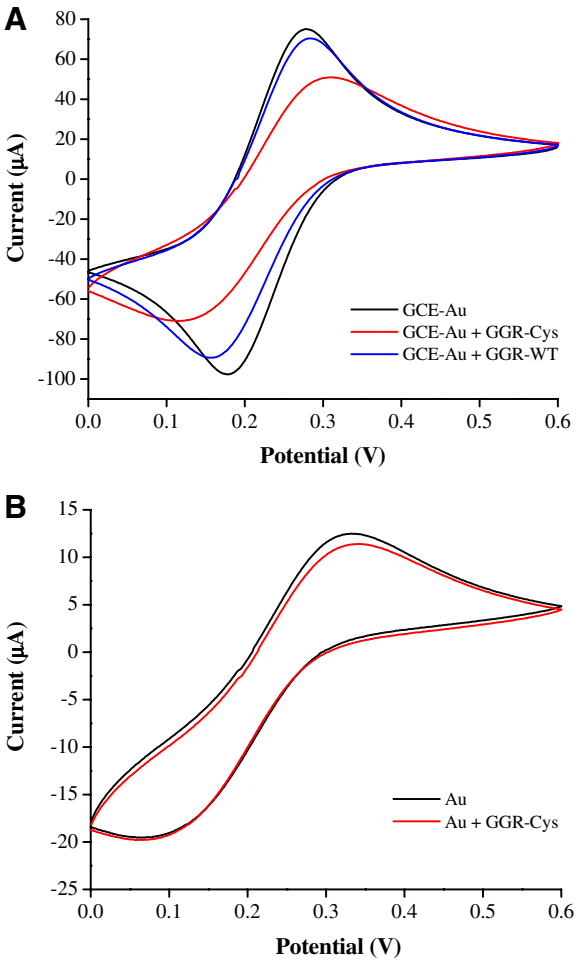

Fig. 6. (A) Cyclic voltammograms of GCE–AuNP electrode before and after modification with GGR–WT and GGR–Cys in 10 mM $K_3Fe(CN)_6$ as redox probe. (B) Cyclic voltammograms of a conventional gold electrode before and after modification with GGR–Cys. Scanning range: 0 to 0.6 V versus Ag/AgCl reference electrode at 50 mV/s.

Detection of glucose

The GCE–AuNPs with GGR–Cys immobilized on the surface were used as a biosensor for the detection of glucose. This system is based on the specificity of the glucose receptor and the ligand-induced conformational change that occurs after glucose binds to the protein. Studies showed that when a ligand binds to a periplasmic binding protein, such as the GGR used in the current work, the protein undergoes a structural change [14]. In previous reports, this effect was studied extensively and confirmed by atomic force microscopy [22], quartz crystal microbalance [15–17,20], and electrochemical impedance spectroscopy [18,21]. It was demonstrated that the flexible ligand-free protein undergoes a conformational change to a more rigid structure after ligand binding [20]. In the current work, after immersion of the GGR–Cys modified electrode in a solution containing glucose, the cyclic voltammogram shows that the oxido/reduction current decreases concurrently with a shift toward more positive potentials (Fig. 7). This is a result of the glucose binding, associated with the closing structure of the protein around its binding pocket, hindering the electron transfer of the redox probe on the active surface of the electrode. These observations are in agreement with previous impedance spectroscopy studies that showed an increase in the electron transfer resistance after glucose binding [18,22]. Fig. 7 shows the cyclic voltammogram of the GCE–AuNP electrode modified with GGR–Cys before and after 5 min incubation with different concentrations of glucose ranging from 0.1 to 1 μM. The decrease in the current was proportional with the glucose concentration. No further decrease in the signal

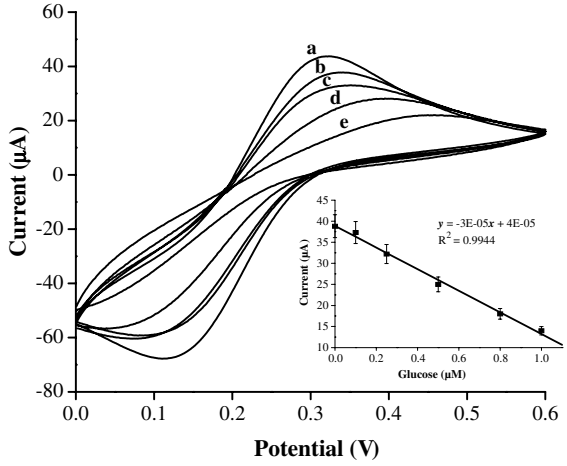

Fig. 7. Cyclic voltammograms of GCE–AuNP electrode modified with GGR–Cys after 5 min incubation with different glucose concentrations: 0 μM (a), 0.1 μM (b), 0.25 μM (c), 0.5 μM (d), and 1 μM (e). Cyclic voltammograms were recorded in 10 mM $K_3Fe(CN)_6$ as redox probe. Scanning range: 0 to 0.6 V versus Ag/AgCl reference electrode at 50 mV/s. Inset: Biosensor calibration curve for glucose. The error bars represent the standard deviation of triplicate measurements obtained with different electrodes.

was obtained at concentrations higher than 1 μM. Increasing the incubation time (e.g., 1 h, 12 h) does not result in a lower detection limit, showing that glucose binding is a nearly immediate effect. The detection limit of the sensor was 0.18 μM, calculated based on the standard deviation and the slope, using the $3\sigma/S$ formula, where σ is the standard deviation of the responses of three blank samples obtained with different electrodes and S is the slope of the calibration curve.

Although in other previous studies we have shown that glucose does not bind to flat gold surfaces [15,17], we did control experiments to check for the possible binding of glucose to the AuNPs. Results showed that incubation of the bare GCE–AuNP electrode in a glucose solution has no effect on the electrochemical current, indicating that binding of the glucose with the immobilized GGR protein on the AuNPs is responsible for the observed decrease of the redox peaks.

When the GCE–AuNP–GGR–Cys electrode was incubated with three other compounds that do not bind GGR (β-D-fructose, L-valine, and L-leucine), no decrease in the electrochemical signal was observed (Fig. 8). These results show that the proposed biosensor specifically binds its target sugar and shows no response to compounds that are not natural ligands.

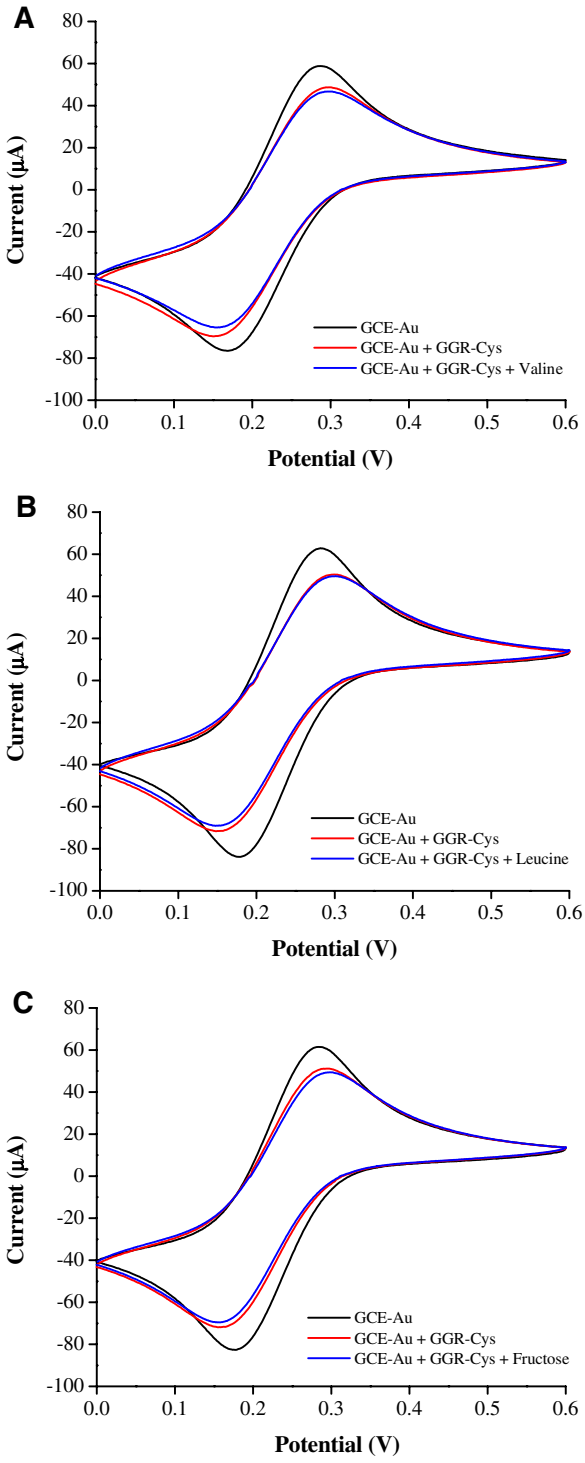

Fig. 8. Binding studies of the GCE–Au–GGR–Cys biosensor for valine (A), leucine (B), and fructose (C) in 10 mM $K_3Fe(CN)_6$ as redox probe. Scanning range: 0 to 0.6 V versus Ag/AgCl reference electrode at 50 mV/s.

Conclusions

We have studied the surface chemistry and interactions of AuNPs with a wild-type and a genetically engineered thiol-containing glucose receptor proteins, and we used this system to construct an electrochemical sensor for selective detection of glucose. The interaction of proteins with AuNPs and the surface chemistry was studied with UV–Vis spectroscopy, TEM, ζ-potential, and PSD analysis, and the results were confirmed with CV. The gold colloids form large aggregates in the presence of the thiol-containing protein. This is due to the strong binding between the gold and the cysteine group that was genetically engineered

in the protein sequence. Under the same experimental conditions (pH, temperature, and buffer solution) but using the WT protein, gold colloids do not aggregate in the same manner. These experiments suggest that the surface-exposed cysteine is key to the binding of the protein to the AuNPs. The electrochemical GGR-based biosensor developed in this work is suitable for selective determination of glucose in the micromolar concentration range, with a detection limit of 0.18 μM. The AuNP reagentless glucose biosensor described here provides a unique addition to the currently available methods to detect glucose. As compared with classical solid gold electrodes, the use of AuNP modified GCE offers several advantages such as a large surface area that provides multiple binding points for proteins (thereby facilitating loading of more protein molecules), high conductivity, and increased sensitivity. The application of this strategy of combined genetic engineering, AuNPs, and electrochemistry serves as a useful tool for the study of receptor–ligand interactions.

Acknowledgments

This work was supported by NSF CTS 0329698 (L.A.L.), U.S. Army Breast Cancer Research Grant Concept Award W81XWH-06-1-0621 (L.A.L.), and U.S. Army W911WF-05-1-0339 (S.A.).

References

[1] C.A. Mirkin, R.L. Letsinger, R.C. Mucic, J.J. Storhoff, A DNA-based method for rationally assembling nanoparticles into macroscopic materials, Nature 382 (1996) 607–609.
[2] O.V. Salata, Applications of nanoparticles in biology and medicine, J. Nanobiotechnol. 2 (2004) 1–6.
[3] N.C. Tansil, Z.Q. Gao, Nanoparticles in biomolecular detection, Nano Today 1 (2006) 28–37.
[4] J.H. Kim, J.S. Kim, H. Choi, S.M. Lee, K.N. Yu, E. Kuk, Y.K. Kim, D.H. Jeong, M.H. Cho, Y.S. Lee, Nanoparticle probes with surface enhanced Raman spectroscopic tags for cellular cancer targeting, Anal. Chem. 78 (2006) 6967–6973.
[5] S. Mandal, S. Phadtare, M. Sastry, Interfacing biology with nanoparticles, Curr. Appl. Physics 5 (2005) 118–127.
[6] S.G. Penn, L. He, M.J. Natan, Nanoparticles for bioanalysis, Curr. Opin. Chem. Biol. 7 (2003) 609–615.
[7] J. Wang, Nanoparticle-based electrochemical bioassay of proteins, Electroanalysis 19 (2007) 769–776.
[8] S. Guo, E. Wang, Synthesis and electrochemical applications of gold nanoparticles, Anal. Chim. Acta 598 (2007) 181–192.
[9] P. Yanez-Sedeno, J.M. Pingarron, Gold nanoparticles-based electrochemical biosensors, Anal. Bioanal. Chem. 382 (2005) 884–886.
[10] I. Willner, R. Baron, B. Willner, Integrated nanoparticle–biomolecule systems for biosensing and bioelectronics, Biosens. Bioelectron. 22 (2007) 1841–1852.
[11] C. Lei, S-Q. Hu, N. Gao, G-L. Shen, R-Q. Yu, An amperometric hydrogen peroxide biosensor based on immobilizing horseradish peroxidase to a nano-Au monolayer supported by sol–gel derived carbon ceramic electrode, Bioelectrochemistry 65 (2004) 33–39.
[12] W. Yang, J. Wang, S. Zhao, Y. Sun, C. Sun, Glucose oxidase/colloidal gold nanoparticles immobilized in Nafion film on glassy carbon electrode: Direct electron transfer and electrocatalysis, Bioelectrochemistry 69 (2006) 158–163.
[13] Y. Hu, A. Das, M.H. Hecht, G. Scoles, Nanografting de novo proteins onto gold surfaces, Langmuir 21 (2005) 9103–9109.
[14] F.A. Quiocho, Atomic structures of perisplasmic binding proteins and the high affinity active transport systems in bacteria, Philos. Trans. R. Soc. Lond. 326 (1990) 341–351.
[15] K.S. Carmon, R.E. Baltus, L.A. Luck, A piezoelectric quartz crystal biosensor: The use of two single cysteine mutants of the periplasmic E. coli glucose/galactose receptor as target proteins for the detection of glucose, Biochemistry 43 (2004) 1429–1456.
[16] K.S. Carmon, R.E. Baltus, L.A. Luck, A biosensor for estrogenic substances using the quartz crystal microbalance, Anal. Biochem. 345 (2005) 277–283.
[17] L.A. Luck, M.J. Moravan, J.E. Garland, B. Salopek-Sondi, D. Roy, Chemisorptions of bacterial receptors for hydrophobic amino acids and sugars on gold for biosensor applications: A surface plasmon resonance study of genetically engineered proteins, Biosens. Bioelectron. 19 (2003) 249–259.
[18] J. Wang, K.S. Carmon, L.A. Luck, I.I. Suni, Electrochemical impedance biosensor for glucose detection utilizing a periplasmic E. coli receptor protein, Electrochem. Solid-State Lett. 8 (2005) H61–H64.
[19] A. Tripathi, J. Wang, L.A. Luck, I.I. Suni, Nanobiosensor design utilizing a periplasmic E. coli receptor protein immobilized within Au/polycarbonate nanopores, Anal. Chem. 79 (2007) 1266–1270.
[20] R.E. Baltus, K.S. Carmon, L.A. Luck, Quartz crystal microbalance with immobilized protein receptors: A comparison of response to ligand binding for direct protein immobilization and protein attachment via a disulfide linker, Langmuir 23 (2007) 3990–3995.
[21] J. Wang, L.A. Luck, I.I. Suni, Immobilization of the glucose–galactose receptor protein onto a Au electrode through a genetically engineered cysteine residue, Electrochem. Solid-State Lett. 10 (2007) 133–136.
[22] I. Sokolov, S. Venkatesh, L.A. Luck, Change in rigidity in the activated form of the glucose/galactose receptor from E. coli: A phenomenon that will be key to the development of biosensors, Biophys. J. 90 (2006) 1058–1063.
[23] R.M. de Lorimier, Y. Tian, H.W. Hellinga, Binding and signaling of surface-immobilized reagentless fluorescent biosensors derived from periplasmic binding proteins, Protein Sci. 15 (2006) 1936–1944.
[24] D. Andreescu, K.S. Tapan, D.V. Goia, Stabilizer free nanosize gold sols, J. Colloid Interface Sci. 298 (2006) 93–100.
[25] C.G. Blatchford, J.R. Campbell, J.A. Creighton, Plasma resonance-enhanced Raman scattering by absorbates on gold colloids: The effects of aggregation, Surf. Sci. 120 (1982) 435.
[26] S. Chah, M.R. Hammond, R.N. Zare, Gold nanoparticles as a colorimetric sensor for protein conformational changes, Chem. Biol. 12 (2005) 323–328.
[27] D. Aili, K. Enander, J. Rydberd, I. Lundstrom, L. Baltzer, B. Lieberg, Aggregation-induced folding of a de novo designed polypeptide immobilized on gold nanoparticles, J. Am. Chem. Soc. 128 (2006) 2194–2195.
[28] P. Yanez-Sedeno, J.M. Pingarron, Gold nanoparticles-based electrochemical biosensors, Anal. Bioanal. Chem. 382 (2005) 884–886.
[29] (a) V.C. Sanz, M.L. Mena, A. Gonzalez-Cortes, P. Yánez-Sedeno, J.M. Pingarron, Development of a tyrosinase biosensor based on gold nanoparticles-modified glassy carbon electrodes – Application to the measurement of a bioelectrochemical polyphenols index in wines, Anal. Chim. Acta 528 (2005) 1;
(b) M.L. Mena, P. Yánez-Sedeno, J.M. Pingarron, A comparison of different strategies for the construction of amperometric enzyme biosensors using gold nanoparticle-modified elctrode, Anal. Biochem. 336 (2005) 20–26.